Ca²⁺ Depletion in the ER Causes Store-Operated Ca²⁺ Entry via the TRPC6 Channel in Mouse Brown Adipocytes

Ryotaro HAYATO[1], Takaya MATSUMOTO[1,2], Yoko HIGURE[1]

[1]Laboratory of Anatomy and Physiology, School of Nutritional Sciences, Nagoya University of Arts and Sciences, Nissin, Aichi, Japan, [2]Laboratory of Nutrition, School of Health and Human Life, Nagoya Bunri University, Inazawa, Aichi, Japan

Summary

β_3-adrenergic activation causes Ca²⁺ release from the mitochondria and subsequent Ca²⁺ release from the endoplasmic reticulum (ER), evoking store-operated Ca²⁺ entry (SOCE) due to Ca²⁺ depletion from the ER in mouse brown adipocytes. In this study, we investigated how Ca²⁺ depletion from the ER elicits SOCE in mouse brown adipocytes using fluorometry of intracellular Ca²⁺ concentration ($[Ca^{2+}]_i$). The administration of cyclopiazonic acid (CPA), a reversible sarcoplasmic/endoplasmic reticulum calcium ATPase (SERCA) pump blocker in the ER, caused an increase in $[Ca^{2+}]_i$. Moreover, CPA-induced SOCE was suppressed by the administration of a Ca²⁺-free Krebs solution and the transient receptor potential canonical 6 (TRPC6) selective blockers 2-APB, ML-9 and GsMTx-4 but not Pico145, which blocks TRPC1/4/5. Administration of TRPC6 channel agonist 1-oleoyl-2-acetyl-sn-glycerol (OAG) and flufenamic acid elicited Ca²⁺ entry. Moreover, our RT-PCR analyses detected mRNAs for TRPC6 in brown adipose tissues. In addition, western blot analyses showed the expression of the TRPC6 protein. Thus, TRPC6 is one of the Ca²⁺ pathways involved in SOCE. These modes of Ca²⁺ entry provide the basis for heat production *via* activation of Ca²⁺-dependent dehydrogenase and the expression of uncoupling protein 1 (UCP1). Enhancing thermogenic metabolism in brown adipocytes may serve as broad therapeutic utility to reduce obesity and metabolic syndrome.

Key words

Brown adipocytes • Endoplasmic reticulum • Transient receptor potential channel • Ca²⁺ signaling • Thermogenesis
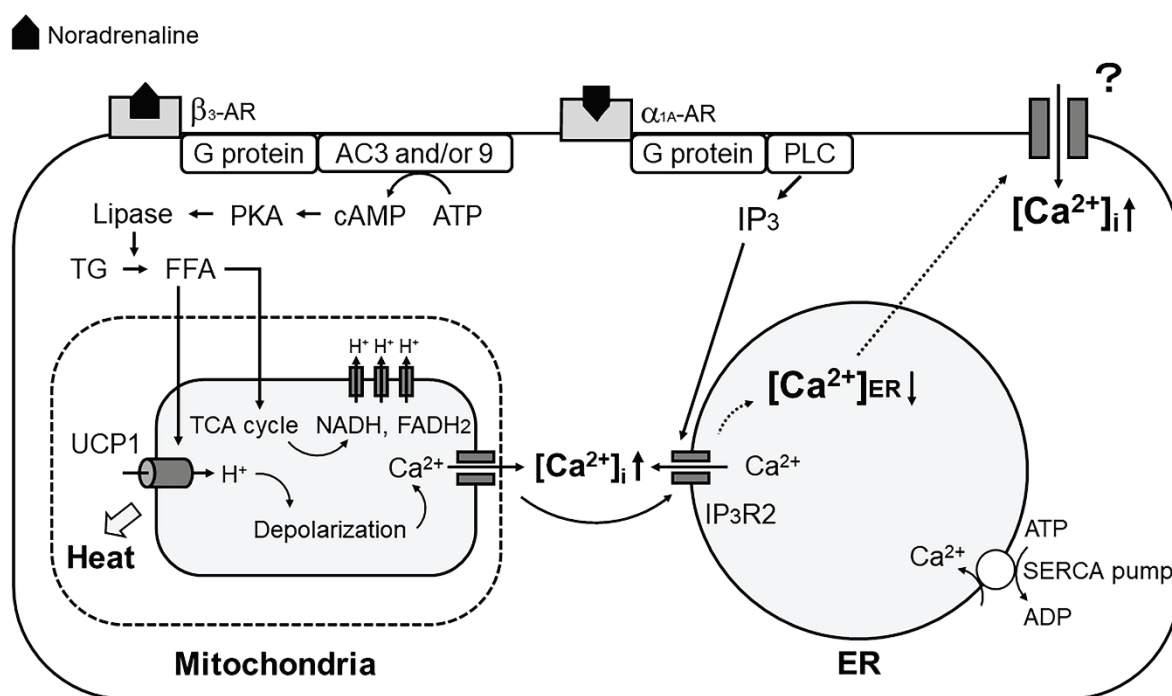
Corresponding author

R. Hayato, Laboratory of Anatomy and Physiology, School of Nutritional Sciences, Nagoya University of Arts and Sciences, 57, Takenoyama, Iwasaki-cho, Nissin-City, Aichi 470-0196, Japan. E-mail: hayato@nuas.ac.jp

Introduction

The functions of cell organelles such as the endoplasmic reticulum (ER) and mitochondria include the provision of a Ca²⁺ supply source and the maintenance of intracellular Ca²⁺ homeostasis [1]. The ER controls the intracellular Ca²⁺ concentration ($[Ca^{2+}]_i$) by responding to physiological stimulation, resulting in the ER release of Ca²⁺ through inositol 1,4,5-trisphosphate (IP₃), leading to store-operated Ca²⁺ entry (SOCE) as a consequence of the loss of Ca²⁺ in the ER [2-5]. Further, mitochondria release Ca²⁺ by the activation of the β_3-adrenergic receptor, thus activating Ca²⁺-induced Ca²⁺ release (CICR), and subsequently eliciting Ca²⁺ entry into brown adipocytes [6]. In low-temperature environments, sympathetic nerves release noradrenaline and activate α_{1A}- and β_3-adrenergic receptors on brown adipocytes (Fig. 1). The activation of the β_3-adrenergic receptor promotes the hydrolysis of triglycerides *via* the production of cyclic adenosine monophosphate (cAMP) and activation of protein kinase A (PKA), leading to enhanced hormone-dependent lipase activity [7,8,9]. Free fatty acids (FFAs) derived from triglycerides, due to the activation of hormone-dependent lipase, enhance the tricarboxylic acid (TCA) cycle and increase the electrochemical potential for H⁺ [9,10]. FFAs also activate uncoupling protein type 1 (UCP1) [11]. This uncoupling leads to heat production [12,13]. During this time, mitochondria release Ca²⁺ due to mitochondrial depolarization by the influx of H⁺ *via* UCP1; this not only

Fig. 1. Adrenergic signaling pathways and their interactions in mouse brown adipocytes. The pathways indicated by the black line arrows represent the processes directly involved in $[Ca^{2+}]_i$ increase. The pathways indicated by the dotted line arrows represent those that activate the processes leading to a rise in $[Ca^{2+}]_i$ due to Ca^{2+} depletion in the ER. Abbreviations: AR, adrenergic receptor; AC, adenylate cyclase; PKA, protein kinase A; cAMP, cyclic adenosine monophosphate; TG, triacylglycerol; FFA, free fatty acid; PLC, phospholipase C; DAG, diacylglycerol; IP$_3$, inositol trisphosphate; IP$_3$R2, IP$_3$ receptor type 2.

activates CICR but also subsequently elicits SOCE into brown adipocytes. Conversely, the activation of the α_{1A}-adrenergic receptor by noradrenaline released from the sympathetic nerve elicits a large phasic rise in $[Ca^{2+}]_i$ *via* Ca^{2+} release from the ER through the IP$_3$ receptor [14-15]. This also leads to the activation of SOCE by the depletion of Ca^{2+} in the ER [6,16-17]. These elevations in $[Ca^{2+}]_i$ stimulate the rate of heat production [18-19].

    A diversity of Ca^{2+}-elevating pathways has been proposed to contribute to Ca^{2+} homeostasis in brown adipocytes. However, the most important Ca^{2+} influx pathway, coupled with Ca^{2+} loss in the ER, is most likely SOCE, identified as a Ca^{2+} influx pathway in various tissues, where it regulates several important physiological functions. The search for channels mediating SOCE led to the identification of mammalian transient receptor potential canonical (TRPC) channels. Various TRPC channels are functionally expressed in brown adipocytes. TRPC1 increases the metabolic performance of brown adipocytes by activating the respiration potential after stimulation with β adrenergic activation [20]. TRPC5 was detected in 3T3-L1 cells, the brown adipocyte cell line derived from fibroblasts, and controls adiponectin secretion [21]. Thus, TRPCs have various roles in brown adipocytes. In mammals, TRPC channels

have been suggested as potential candidates for mediating SOCE in various tissues [22-24]. Therefore, we aimed to determine whether activation or inhibition of TRPC channels affects SOCE in mouse brown adipocytes. In this study, we found that SOCE in mouse brown adipocytes was elicited by the activation of TRPC6 channels due to Ca^{2+} depletion in the ER. We discuss the underlying mechanism that allows TRPC6 to elicit Ca^{2+} entry and the role of TRPC6 in thermogenesis. These modes of Ca^{2+} entry provide the basis for heat production *via* the activation of Ca^{2+}-dependent dehydrogenase and the expression of uncoupling protein 1 (UCP1). Therefore, promoting thermogenic metabolism in brown adipocytes is expected to have broad therapeutic use in reducing obesity and metabolic syndrome.

Methods

Animals

    Four-week-old male C57BL/6J mice were obtained from Japan SLC (Shizuoka, Japan) and were kept at 25-27 °C for 3-5 h with free access to food and water. They were anesthetized with isoflurane and sacrificed by cervical dislocation, the interscapular brown

adipose tissues were isolated. All experiments were performed following the guiding principles for the care and use of Animals in the Field of Physiological Sciences and were approved by the Council of the Physiological Society of Japan and the Animal Institutional Review Board of Nagoya University of Arts and Sciences.

Cell isolation and primary culture

The preparations and solutions are described in a previous study [6,17]. Brown adipose tissues were briefly isolated from mice interscapular regions; other tissues, such as neurons and muscles, were surgically eliminated, and the brown adipose tissues were treated with type-2 collagenase. The isolated brown adipocytes were cultured on 35 mm poly-L-lysine-coated glass-bottom culture dishes for 3-7 days, supplemented with 10 % fetal bovine serum and 1 % penicillin-streptomycin at 37 °C in a humidified 10 % CO_2 incubator. After culturing, the adipocytes were used for Ca^{2+} imaging.

Ca^{2+} imaging and the analysis of $[Ca^{2+}]_i$

Mouse brown adipocytes cultured on glass-bottom dishes were loaded with 5 μM fura-2 acetoxymethyl ester (fura-2 AM) and incubated for 45 min at 37 °C. Changes in $[Ca^{2+}]_i$ in the adipocytes were measured using a conventional Ca^{2+}-imaging system (CMOS camera, ORCA-Spark, Hamamatsu Photonics, Shizuoka, Japan) set on an inverted microscope (ECLIPSE Ti with an objective, 40× water, numerical aperture 1.15, NIKON, Tokyo, Japan). Fura-2-stained brown adipocytes were excited alternatively at 340 nm and 380 nm using an illumination system pE-300ultra (CoolLED Limited, Andover, UK) with the inverted microscope. Fura-2 fluorescence was recorded using a bandpass filter (D535/30, Chroma Technology Corp., Vermont, USA). This fluorescence intensity was averaged over the contour of each cell using image acquisition at intervals of once every 10-30 s and calculated $[Ca^{2+}]_i$ in using software (HCImage, Hamamatsu Photonics, Shizuoka, Japan) in single-cell culture experiments. Regions of interest were set for the whole cells of every brown adipocyte recorded in the images and analyzed. We obtained $[Ca^{2+}]_i$ of 5-30 cells in a single measurement.

RNA isolation and RT-PCR

Total RNA was extracted from brown adipose tissues, brains, and skeletal muscles isolated from 4-week-old mice under anesthesia. Samples were homogenized in 150 μl of ISOGEN II (QIAGEN, Germany) at 20000 rpm using an ultrasonic homogenizer (DIAX 100, Heidolph, Germany). Next, 60 μl of RNase free water (Takara Bio, Japan) was added, and the samples were mixed for 15 s. After incubation at 25 °C for 10 min, the samples were centrifuged for 15 min at 14000 rpm using a benchtop centrifuge (MiniSpin+, Eppendorf, Germany). The upper aqueous phase was collected, 0.75 μl p-bromoanisole was added, and the solution was gently mixed for 15 s. After incubation at 25 °C for 5 min, the samples were centrifuged at 14000 rpm for 10 min and the upper aqueous phase was collected. An equal volume of 2-propanol was added to the volume of upper aqueous phase collected and samples were gently mixed with 4 μl Dr. GenTLE (Takara Bio, Japan) and 10 μl 3 M sodium acetate. After incubation at 25 °C for 10 min, the samples were centrifuged at 14000 rpm for 10 min and the upper aqueous phase was removed. After adding 0.5 ml 75 % (v/v) ethanol and centrifuging at 10000 rpm for 3 min, the upper aqueous phase was removed. This step was repeated twice, after which the sample was dried and allowed to precipitate. After precipitation, 20 μl of RNase free water was added, and the sample was stored at -20 °C.

Reverse transcription was performed using the OneStep RT-PCR Kit (QIAGEN) according to the manufacturer's recommendations. The resulting cDNA was stored at -20 °C and used for standard PCR. Thereafter, 1 μl of the cDNA reaction mixture was added to 9 μl of the PCR reaction mixture and 1.25 μl of each primer. The sense and antisense oligonucleotide primers specific for TRPC6 channel subtypes were 5'-AAAGAT-ATCTTCAAATTCATGGTC-3' and 5'-CACGTCCGC-ATCATCCTCAATTTC-3', respectively. We used primers specific for β-actin as the positive control and H_2O as a negative control. The following primers for β-actin were used: 5'-GGCTGTATTCCCCTCCATCG-3'; antisense, 5'-CCAGTTGGTAACAATGCCATGT-3'. Each cDNA fragment was amplified in a DNA thermal cycler (GeneAtlas G02, ASTEC, Japan). The PCR conditions were as follows: initial denaturation at 95 °C for 15 min, followed by 35 cycles of denaturation at 94 °C for 30 s, annealing at 60 °C for 1 min, extension at 72 °C for 90 s, and a final extension at 72 °C for 10 min. The PCR products were electrophoresed on a 2 % (w/v) agarose gel, stained with ethidium bromide (0.1 μg/ml), and visualized under ultraviolet illumination.

Protein isolation and Western blotting analysis

Brown adipose tissues, brains, and skeletal muscles were homogenized in 20 mM Tris buffer

(pH 7.4) containing 1 mM ethylene glycol-bis(2-amino-ethylether)-N,N,N,N'-tetraacetic acid (EGTA) and protease inhibitors (Roche Diagnostics, Indiana, USA) using a homogenizer (DIAX 100, Heidolph, Germany) at 15000 rpm and 4 °C for 1 min. Next, the samples were centrifuged at 25000 rpm and 4 °C for 60 min. After removing the supernatant, including the lipid fraction, the precipitate was placed in 1 ml Tris-EDTA (TE) buffer. Precipitated fractions were denatured, separated by sodium dodecyl sulfate-polyacrylamide gel electrophoresis (SDS-PAGE), and calibrated with pre-stained protein molecular weight markers (Bio-Rad, California, USA). The separated proteins were transferred onto nitrocellulose membranes (Hybond-C, Bio-Rad) and blocked with 5 % (w/v) BSA in Tris-buffered saline (TBS) and 0.1 % Tween-20 (Sigma-Aldrich, St. Louis, Missouri, USA). The nitrocellulose membranes were stained with affinity-purified rabbit polyclonal antibodies (1:500) specific for TRPC6 (Alomone Labs, Jerusalem, Israel) at 20 °C for 1 h and then at 4 °C overnight. After two washes with TBS for 10 min, the membranes were stained with anti-rabbit horseradish peroxidase (HRP)-conjugated IgG (1:10000) for 1 h. The presence of TRPC6 channel proteins was detected using an enhanced luminol-linked chemical luminescence detection system (Amersham, New Jersey, USA).

Drugs and materials

Fetal Bovine Serum, penicillin-streptomycin, and Dulbecco's Modified Eagle Medium (DMEM) (low glucose type) were purchased from Thermo Fisher Scientific (Massachusetts, USA). Collagenase type-2 (class 2) was obtained from Worthington Biochemical (New Jersey, USA), and DNase-I was obtained from Roche Diagnostics (Indiana, USA). Poly-L-lysine was obtained from Merck (Darmstadt, Germany). Glass-bottom culture dishes were obtained from Matsunami Glass Industry Co. (Osaka, Japan). Cyclopiazonic acid (CPA), ML-9, and bovine serum albumin (BSA) were obtained from Sigma-Aldrich (St. Louis, MO, USA). Flufenamic acid was purchased from Wako Pure Chemical Industries, Ltd. (Saitama, Japan); 1-oleoyl-2-acetyl-sn-glycerol (OAG) was purchased from Funakoshi Co. Ltd. (Tokyo, Japan). GsMTx-4 was purchased from Peptide Institute, Inc. (Osaka, Japan). All agonists and antagonists were used at a concentration of >2-10 times the EC_{50} and IC_{50} of TRPC6. Primers for RT-PCR were obtained from Eurofins Genomics, Inc. (Tokyo, Japan). Fura-2 AM was purchased from DOJINDO Laboratories

(Kumamoto, Japan). Anti-TRPC6 antibodies and their blocking peptides were purchased from Alomone Laboratories (Jerusalem, Israel).

Solutions

The control Krebs saline solution comprised 150 mM NaCl, 5 mM KCl, 2 mM $CaCl_2$, 0.5 mM $MgCl_2$, 10 mM HEPES, and 5 mM glucose (pH 7.4, adjusted with NaOH). The Ca^{2+}-free Krebs solution was prepared using isomolar Na^+ in the control Krebs saline solution. Drugs were applied by substituting the perfusing solution with a solution containing the drug(s). The solution perfusion rate was maintained at 5 ml/min using a peristaltic pump (PST-100N, AGC Techno Glass Co., Ltd., Shizuoka, Japan). The solution concentration reached a peak within 3 min. Agonists, including CPA, OAG, and flufenamic acid, and blockers, including 2-APB and ML-9, were dissolved in dimethyl sulfoxide and stored at -20 °C before use. GsMTx-4 was dissolved in water and stored at -20 °C before use.

Statistical analyses

Differences in the activation or inhibition of $[Ca^{2+}]_i$ by the administration of drugs were analyzed using one-way analysis of variance (ANOVA). Calculations were performed with EZR software produced by the Jichi Medical University Saitama Medical Center (Saitama, Japan) [25]. Differences with P values<0.05 were considered statistically significant. Assuming a confidence interval of 95 %, we calculated the acceptable error as 1.96× standard error (SE). In our experiments, the SE of CPA-induced rises in $[Ca^{2+}]_i$ was ± 15.4 nM. Therefore, we acquired approximately >30 cells of $[Ca^{2+}]_i$ data elicited by CPA.

Results

Ca^{2+} release from the ER by blocking the Ca^{2+} pump activates Ca^{2+} entry

Administration of 10 μM cyclopiazonic acid (CPA) (a reversible ER Ca^{2+} pump blocker) caused an increase in $[Ca^{2+}]_i$ (Fig. 2). The increase in $[Ca^{2+}]_i$ reached a plateau of 198.2 ± 15.4 nM (mean ± SE, 67 cells measured from 5 individual cultures, 3 mice). While extracellular Ca^{2+} was removed during the maintained $[Ca^{2+}]_i$ rise induced by the application of CPA, the increase in $[Ca^{2+}]_i$ level was decreased to the initial basal level. These results indicated that CPA-induced Ca^{2+} rises consist of a Ca^{2+}-entry

component in mouse brown adipocytes. The magnitude of the net reduction of the $[Ca^{2+}]_i$ level was 216.2 ± 17.2 nM (mean $\pm$ SE, 67 cells measured from 5 individual cultures, 3 mice) from the level before the perfusion of Ca^{2+}-free Krebs solution in mouse brown adipocytes.

Involvement of the activation of TRP channels in the CPA-induced Ca^{2+} rise

To test the involvement of TRPC channel activation in CPA-induced Ca^{2+} entry, we recorded the effects of TRPC6 channel blockers on the rise in Ca^{2+} levels. TRP channel modulation by the administration of 2-aminoethoxydiphenyl borate (2-APB) includes activation of TRPV1, TRPV2, TRPV3, TRPA1, and TRPM6 and inhibition of TRPM2, TRPM7, TRPC1, TRPC3, TRPC5, TRPC6, and TRPC7 [26-31]. The administration of 30 μM 2-APB inhibited the Ca^{2+} entry evoked by 10 μM CPA (Fig. 3A-B). The magnitude of the net reduction in the $[Ca^{2+}]_i$ level was 157.9 ± 10.3 nM (mean $\pm$ SE, 117 cells measured from 7 individual cultures, 4 mice) from the level before perfusion of the 2-APB solution. Interestingly, in 71 % of the mouse brown adipocytes, we recorded the enhancement of Ca^{2+} entry by the administration of 30 μM 2-APB among CPA-induced Ca^{2+} rises (Fig. 3A, black arrowhead). The magnitude of net elevation of the $[Ca^{2+}]_i$ level was 50.5 ± 3.2 nM (mean $\pm$ SE, 83 cells measured from 7 individual cultures, 4 mice). To further investigate which TRP channel is related to SOCE in mouse adipocytes, we examined the effects of two specific TRPC6 channel blockers, ML-9 and GsMTx-4. ML-9 is the blocker known to rapidly inhibit the TRPC6 channel and enhance the TRPC7 channel [32]. The peptide GsMTx-4, isolated from the venom of the tarantula *Grammostola spatulata*, is a selective inhibitor of stretch-activated cation channels and TRPC6 [33]. As demonstrated in Fig. 3C-F, external administration of 30 μM ML-9 or 10 μM GsMTx-4, which were selective blockers for TRPC6, reduced the amplitude of CPA-evoked Ca^{2+} increases. The magnitude of the net reduction of the $[Ca^{2+}]_i$ level due to the administration of 30 μM ML-9 solution was 140.9 ± 9.3 nM (mean $\pm$ SE, 75 cells measured from 5 individual cultures, 3 mice; Fig. 3C), while that due to the administration of 10 μM GsMTx-4 solution was 61.6 ± 4.1 nM (mean $\pm$ SE, 49 cells measured from 9 individual cultures, 3 mice; Fig. 3E). Wolfrum *et al.* and Sukumar *et al.* reported that brown adipocytes express TRPC1 and TRPC5 and play

physiological roles [20,21]. Therefore, we examined whether TRPC1 or TRPC5 activation affects SOCE upon administration of Pico145, a TRPC1/4/5 selective blocker. However, 100 nM Pico145 did not affect the SOCE elicited by CPA (Fig. 3G, H).

TRPC6 channel agonist activated Ca^{2+} rises in mouse brown adipocytes

CPA causes Ca^{2+} entry *via* TRPC6 channels due to Ca^{2+} depletion in the ER. Hence, direct activation of TRPC6 should elevate $[Ca^{2+}]_i$ in mouse brown adipocytes. OAG, an agonist of TRPC6 channels, was tested to determine whether TRPC6 channels are involved in the $[Ca^{2+}]_i$ increases. The OAG is also a membrane-permeable diacylglycerol (DAG) analog [34]. The extracellular administration of 100 μM OAG induced an increase in $[Ca^{2+}]_i$ (Fig. 4A, B). The magnitude of the net elevation of $[Ca^{2+}]_i$ was 167.7 ± 15.1 nM (mean $\pm$ SE, 60 cells measured from 5 individual cultures, 4 mice) from the basal level. Next, we investigated the pharmacological agent flufenamic acid, which is a non-steroidal anti-inflammatory agent belonging to the family of fenamates and has also been shown to affect the TRPC6 channel protein [35,36], increasing permeability through TRPC6 channels and elevate $[Ca^{2+}]_i$ and inhibiting permeability through TRPC3 but not affect TRPC7 channels [36]. The administration of a selective agonist, 100 μM flufenamic acid, induced an increase in $[Ca^{2+}]_i$ (Fig. 4C, D). The magnitude of the net elevation of the $[Ca^{2+}]_i$ level was 95.6 ± 6.2 nM (mean $\pm$ SE, 46 cells measured from 5 individual cultures, 3 mice) from the basal level.

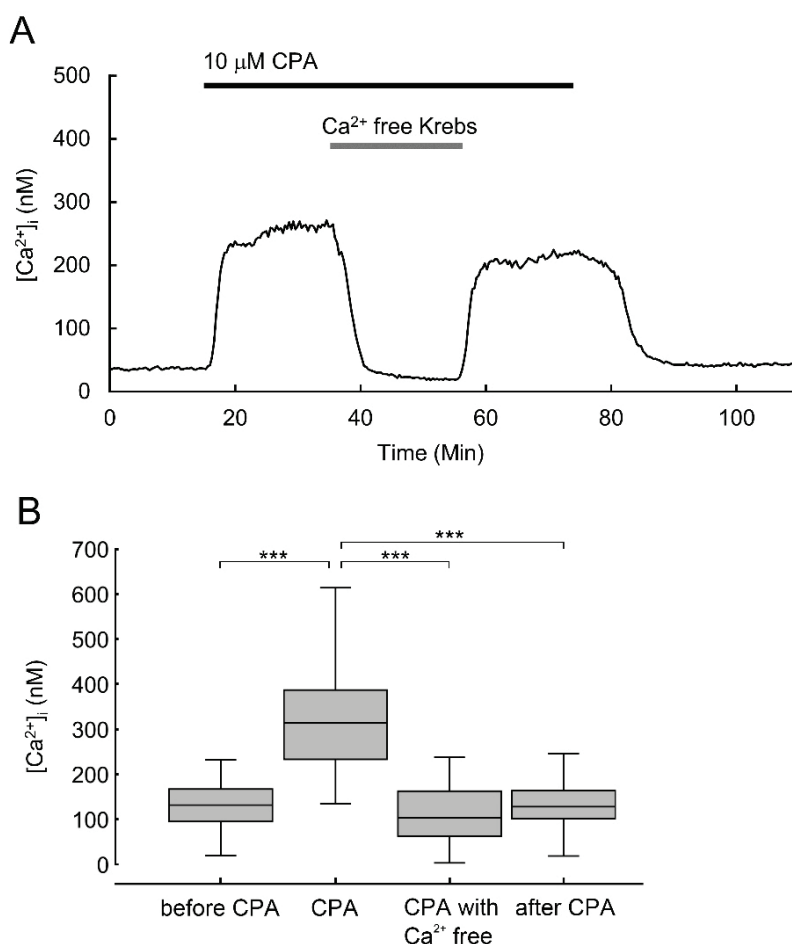*H$^+$ inhibition of SOCE in mouse brown adipocytes*

It is known that TRPC6 channel permeability is inhibited by low pH conditions and enhanced by high pH conditions; however, TRPC5 channel permeability is potentiated by low pH conditions and inhibited by high pH conditions [37]. Therefore, we tested the effects of Krebs solution at pH 7.0 or 7.8 on SOCE in mouse brown adipocytes to clarify whether SOCE occurred by TRPC5 or TRPC6 activation. The administration of 10 μM CPA increased the $[Ca^{2+}]_i$ levels. Decreasing the extracellular pH from 7.4 to 7.0 during Ca^{2+} entry elicited by CPA led to significant decreases (Fig. 5A, B). The magnitude of the net reduction of $[Ca^{2+}]_i$ upon administration of pH 7.0 Krebs solution was 93.7 ± 9.2 nM (mean $\pm$ SE, 33 cells measured from 6 individual cultures, 3 mice) from the basal level. Responses occurred immediately after

changing the extracellular pH and reversibly upon returning to the standard Krebs solution (pH 7.4). Next, we examined intermediate pH values from 7.4 to 7.8 (Fig. 5C, D). Increasing the extracellular pH from 7.4 to 7.8 during Ca^{2+} entry elicited by CPA led to significant increases. The magnitude of the net elevation of $[Ca^{2+}]_i$ upon administration of pH 7.8 Krebs solution was 62.4 ± 14.5 nM (mean $\pm$ SE, 31 cells measured from 8 individual cultures, 3 mice) from the basal level. These results showed that mouse brown adipocytes functionally expressed TRPC6 and it is involved in SOCE.
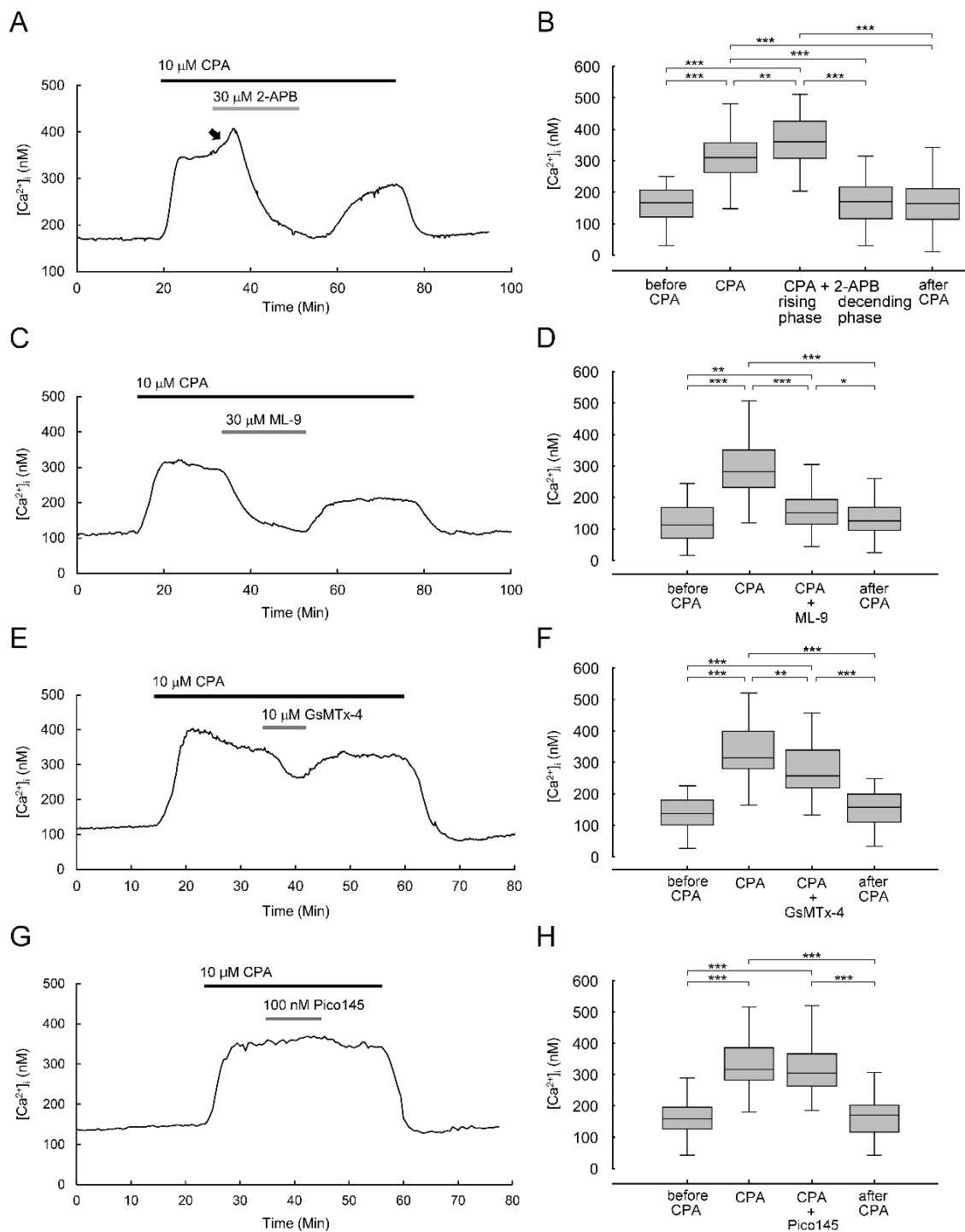
Detection of mRNA and protein of TRPC6

Further experiments were conducted to confirm that the *TRPC6* channel was expressed in brown adipocytes. We detected TRPC6 mRNA expressed on
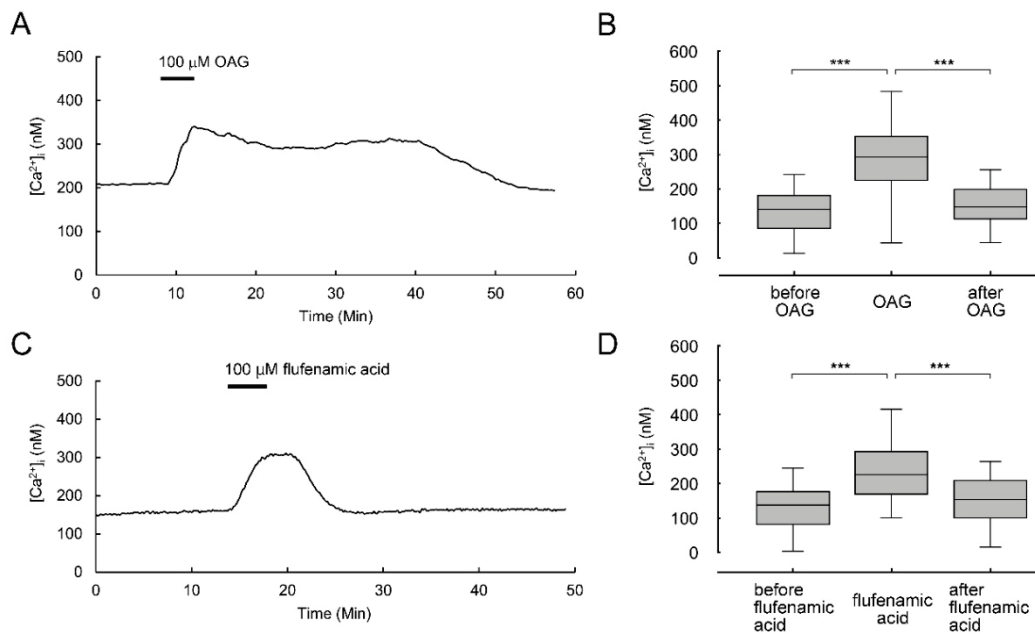
mouse brown adipocytes using excised brown fat tissue to eliminate other tissues such as neurons and muscle by RT-PCR. TRPC6 subtype was successfully amplified from the cDNA using the primer sets (Fig. 6A, B), and western blotting (Fig. 6C) results revealed the presence of TRPC6 in the mouse brown adipocytes. We used a brain protein as a positive control and a skeletal muscle as a negative control. TRPC6 is expressed in mouse brain neurons and has various functions in neurite outgrowth [38], synapse formation [39], and neuronal survival [40] during brain development. Moreover, TRPC6 was not detected in mouse skeletal muscle [41]. We also did not detect TRPC6 protein in mouse skeletal muscle in the present study. The detection of the *TRPC6* subtype mRNA and protein on brown adipocytes agreed with our Ca^{2+} imaging analysis.

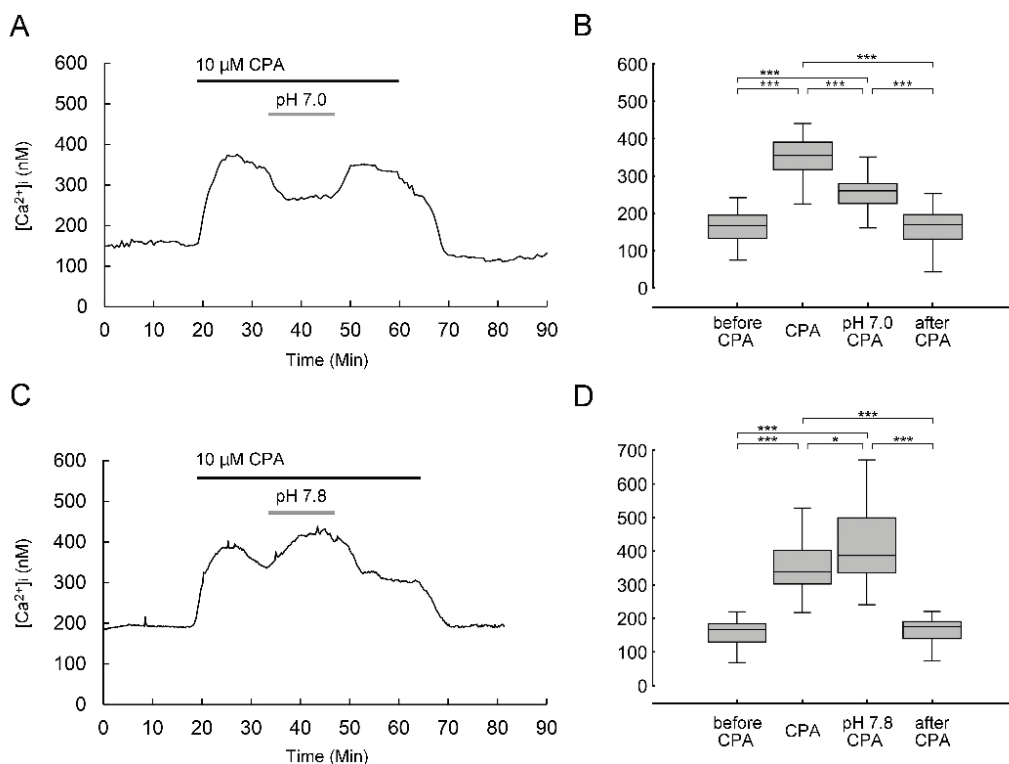**Fig. 2.** Ca^{2+} liberation from the ER by Ca^{2+} pump blocker activates Ca^{2+} entry. (**A**) The administration of 10 μM CPA, a reversible ER Ca^{2+} pump blocker, caused an increase in $[Ca^{2+}]_i$ (black horizontal bar). Removal of external Ca^{2+} quickly and reversibly reduced CPA-induced $[Ca^{2+}]_i$ increase to a level lower than the initial basal level (gray horizontal bar). This figure illustrates the time course of a representing cell. (**B**) Box plots. ANOVA-one way of repeated measures followed by Tukey's *post hoc* test was used to verify differences between the phases (*** P<0.001). Abbreviations: CPA: cyclopiazonic acid; ER: endoplasmic reticulum.

Fig. 3. Depression of CPA-induced $[Ca^{2+}]_i$ is alleviated by 2-APB, ML-9, and GsMTx-4, but not Pico145. The CPA-induced $[Ca^{2+}]_i$ increase was suppressed by 2-APB, ML-9, or GsMTx-4, blockers of TRPC6. (**A**) CPA-induced $[Ca^{2+}]_i$ rises were suppressed by 2-APB. CPA (10 μM) was applied during the period indicated by a black horizontal bar and 2-APB (30 μM) during a gray horizontal bar. The black arrow indicates the component of Ca^{2+} increase due to the administration of 2-APB. (**B**) Box plots. ANOVA-one way of repeated measures followed by Tukey's *post hoc* test was used to verify differences between the phases (** $P<0.01$; *** $P<0.001$). (**C**) CPA-induced $[Ca^{2+}]_i$ rises were inhibited by ML-9. This figure illustrates the time course of a representing cell. CPA (10 μM) was applied during a black horizontal bar, and ML-9 (30 μM) was applied during a gray horizontal bar. (**D**) Box plots. ANOVA-one way of repeated measures followed by Tukey's *post hoc* test was used to verify differences between the phases (* $P<0.05$; ** $P<0.01$; *** $P<0.001$). (**E**) CPA-induced $[Ca^{2+}]_i$ rises were inhibited by GsMTx-4. This figure illustrates the time course of a representing cell. CPA (10 μM) was applied during a black horizontal bar and GsMTx-4 (10 μM) was applied during a gray horizontal bar. (**F**) Box plots. ANOVA-one way of repeated measures followed by Tukey's *post hoc* test was used to verify differences between the phases (** $P<0.01$; *** $P<0.001$). (**G**) CPA-induced $[Ca^{2+}]_i$ increase was not inhibited by Pico145. This figure illustrates the time course of a representing cell. CPA (10 μM) was applied during a black horizontal bar, and Pico145 (100 nM) was applied during a gray horizontal bar. (**H**) Box plots. ANOVA-one way of repeated measures followed by Tukey's *post hoc* test was used to verify differences between the phases (*** $P<0.001$). Abbreviations: CPA: cyclopiazonic acid; 2-APB: 2-aminoethoxydiphenyl borate.
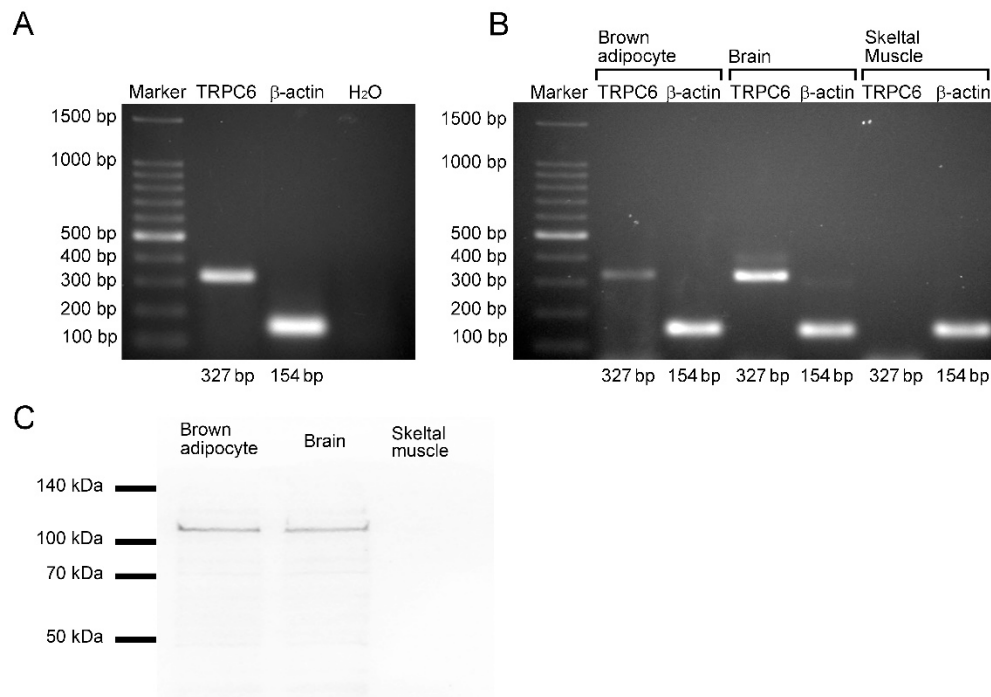
Fig. 4. $[Ca^{2+}]_i$ rises induced by TRPC6 agonists OAG and flufenamic acid. A TRPC6 agonist, OAG (1-oleoyl-2-acetyl-sn-glycerol), elicits $[Ca^{2+}]_i$ increases in mouse brown adipocytes. (**A**) Ca^{2+} increase induced by OAG (100 μM) administration during the period indicated by the black horizontal bars. This figure illustrates the time course of a representing cell. (**B**) Box plots. ANOVA-one way of repeated measures followed by Tukey's *post hoc* test was used to verify differences between the phases (*** P<0.001). (**C**) A TRPC6 selective agonist flufenamic acid elicits an increase in $[Ca^{2+}]_i$ in mouse brown adipocytes. Flufenamic acid (100 μM) was administered during the period indicated by the black horizontal bars. This figure illustrates the time course of a representing cell. (**D**) Box plots. ANOVA-one way of repeated measures followed by Tukey's *post hoc* test was used to verify differences between the phases (*** P<0.001). Abbreviations: OAG: 1-oleoyl-2-acetyl-sn-glycerol.

Fig. 5. The pH dependence of $[Ca^{2+}]_i$ rises elicited by CPA. The pH dependence of SOCE by the administration of 10 μM CPA. (**A**) A reduction in pH from 7.4 to 7.0 led to a decrease in $[Ca^{2+}]_i$ increase in response to 10 μM CPA. This figure illustrates the time course of a representing cell. (**B**) Box plots. ANOVA-one way of repeated measures followed by Tukey's *post hoc* test was used to verify differences between the phases (*** P<0.001). (**C**) A rise in pH from 7.4 to 7.8 led to an elevation in $[Ca^{2+}]_i$ in response to 10 μM CPA. This figure illustrates the time course of a representing cell. (**D**) Box plots. ANOVA-one way of repeated measures followed by Tukey's *post hoc* test was used to verify differences between the phases (* P<0.05; *** P<0.001).

Fig. 6. RT-PCR and Western blotting analysis on mouse brown adipocytes. (**A**) RT-PCR analysis on mouse brown adipocytes. Oligonucleotide primers specific for *TRPC6* were run in separate reactions, and the products were separated using agarose gel electrophoresis. The numerals on each line indicate the expected product size. Oligonucleotide primers specific for *β-actin* were used as positive control. H$_2$O used as a negative control. (**B**) RT-PCR analysis on mouse brown adipocytes, brain, and skeletal muscle. (**C**) Western blotting analysis on mouse brown adipocytes. We detected TRPC6 channel proteins in mouse brown adipocytes and brain but not in mouse skeletal muscle.

Discussion

The present study shows that mouse brown adipocytes functionally express *TRPC6* and partake in SOCE. In Ca^{2+}-imaging studies, CPA evoked Ca^{2+} rises, and the removal of external Ca^{2+} by the administration of Ca^{2+}-free Krebs solution completely inhibited Ca^{2+} entry (Fig. 2). These Ca^{2+} increases were also inhibited by blockers of the selective TRPC6 channels, such as ML-9 or GsMTx-4 (Fig. 3C-F), but not by Pico145, a TRPC1/4/5 blocker (Fig. 3G-H). RT-PCR and western blotting analysis indicated that mRNA and TRPC6 proteins exist in mouse brown adipocytes (Fig. 6). These results indicate that brown adipocytes express TRPC6 channels and have a mechanism for SOCE due to TRPC6 activation. Ca^{2+} imaging also showed that OAG administration evoked Ca^{2+} increases in mouse brown adipocytes (Fig. 4). A study reported that mouse brown adipocytes express the α_{1A}-adrenergic receptor, which couples with the Gq protein [42]. Activation of the Gq protein promotes phospholipase C (PLC) activity, which generates DAG and IP$_3$. IP$_3$ mobilizes Ca^{2+} from the ER, leading to Ca^{2+} loss in the ER, activation of TRPC6, and Ca^{2+} entry.

Simultaneously, DAG produced by PLC activation can directly gate TRPC6. The results shown in this experiment indicate that TRPC6 functions as a SOCE channel and a non-capacitive Ca^{2+} entry channel. Wolfrum *et al.* and Sukumar *et al.* reported that brown adipocytes expressed TRPC1 and TRPC5 [20,21]. Therefore, we tested the effect of the administration of the TRPC1/4/5 selective blocker, Pico145, on CPA-induced Ca^{2+} entry. However, Pico145 did not affect CPA-induced Ca^{2+} entry (Fig. 3G, H). This result suggests that TRPC1 and TRPC5 activation do not cause CPA-induced Ca^{2+} entry. We observed the effects of low-pH and high-pH Krebs solutions on CPA-induced Ca^{2+} entry (Fig. 5). In the low-pH Krebs solution, CPA-induced Ca^{2+} entry was inhibited; in the high-pH Krebs solution, CPA-induced Ca^{2+} entry was potentiated. These results differ from those of TRPC5 and are consistent with those of TRPC6. These results indicate that CPA-induced Ca^{2+} entry is controlled by the activation of TRPC6, not TRPC1 or TRPC5.

In these experiments, we observed a long-lasting Ca^{2+} elevation upon CPA administration. Interestingly, we also observed such a long-term elevation of Ca^{2+} upon administration of the β_3 adrenoceptor agonist BRL37344

[6]. In brown adipocytes, short-term stimulation of the β_3 adrenoceptor (1-3 min) causes approximately 2 h of Ca^{2+} elevation. Long-term elevation of Ca^{2+} concentrations may be toxic owing to the elicitation of apoptotic cell death. However, a prolonged elevation in $[Ca^{2+}]_i$ is necessary for brown adipocytes to continuously produce heat and warm the entire body of the organism [18]. In such cases, continuous excitation of the β signaling is needed, but long-term excitation of the sympathetic nerve is detrimental to life support. Mice are hibernating animals. Continuous excitation of the sympathetic nervous system during hibernation leads to arousal, which causes the individual's death in winter. Therefore, we hypothesize that brown adipocytes allow a continuous increase in Ca^{2+} concentration to produce heat for a long period, even with brief adrenergic stimulation. Therefore, brown adipocytes may tolerate prolonged increases in Ca^{2+} concentration compared to other cells.

We showed that the Ca^{2+} rise elicited by CPA was initially enhanced by the administration of 2-APB, after which the continuous administration of 2-APB reduced the Ca^{2+} rise (Fig. 3A, B). We observed two types of reactions by the administration of 2-APB: (i) the components of Ca^{2+} increase and decrease, and (ii) 2-APB not only blocked TRPM2, TRPM7, TRPC1, TRPC3, TRPC5, TRPC6, and TRPC7 but also activated TRPA1, TRPV1, TRPV2, TRPV3, and TRPM6 channels [26-31]. These results suggest that mouse brown adipocytes express at least two types of TRP channels. Bishnoi *et al.* (2013) and Sun *et al.* (2016) reported that TRPV2 expressed in brown adipocytes contributed to differentiation and thermogenesis [43,44]. The components of Ca^{2+} rise elicited by 2-APB may consist of the activation of TRPV2, and the components of reduction elicited by 2-APB consist of the inhibition of TRPC6.

Under cold exposure, noradrenaline activates the α_{1A} adrenergic receptors, which elicits a large phasic rise in $[Ca^{2+}]_i$ *via* Ca^{2+} release from the ER and subsequently activates SOCE *via* TRPC6. In addition, noradrenaline activates the β_3 adrenergic receptors. This activation causes mitochondrial Ca^{2+} release [6]. The Ca^{2+} released from the mitochondria further elicits CICR from the ER *via* IP$_3$ receptors under the action of IP$_3$ produced by PLC activation and subsequently activates SOCE *via* TRPC6. Thus, brown adipocytes would be able to sustain long-lasting $[Ca^{2+}]_i$ rises due to these modes of sequential activation of Ca^{2+} releases from the mitochondria and the ER and Ca^{2+} entries elicited by adrenergic activation.

Intracellular Ca^{2+} enhances thermogenesis and oxygen consumption in brown adipocytes [18,19]. We demonstrated Ca^{2+} responses by the activation of TRPC6. Interestingly, TRPC6 channels are known to be mechano-sensitive [45]. Indeed, we observed that the $[Ca^{2+}]_i$ rises in response to mechanical stimulation by the water pressure administration of normal Krebs solution on cultured mouse brown adipocytes (unpublished observation). These results indicate that TRPC6 channels may be involved in non-shivering and shivering thermogenesis in brown adipocytes. We assume that Ca^{2+} entry *via* TRPC6 contributes to heat production in mouse brown adipocytes. On this basis, future efforts should be made to characterize TRPC6 channels as a mechanical sensor and to study TRPC6 contribution to the thermogenesis of brown adipocytes in mice.

Conflict of Interest

There is no conflict of interest.

Acknowledgements

References

1. Carafoli E. Intracellular calcium homeostasis. Annu Rev Biochem 1987;56:395-433. https://doi.org/10.1146/annurev.bi.56.070187.002143
2. Berridge MJ. Inositol trisphophate and calcium signalling. Nature 1993;361:315-325. https://doi.org/10.1038/361315a0
3. Hoth M, Penner R. Depletion of intracellular calcium stores activates a calcium current in mast cells. Nature 1992;355:353-356. https://doi.org/10.1038/355353a0
4. Parekh AB. Store-operated Ca^{2+} entry: dynamic interplay between endoplasmic reticulum, mitochondria, and plasma membrane. J Physiol 2003;547:333-348. https://doi.org/10.1113/jphysiol.2002.034140
5. Putney JW Jr. A model for receptor-regulated calcium entry. Cell Calcium 1986;7:1-12. https://doi.org/10.1016/0143-4160(86)90026-6

6.   Hayato R, Higure Y, Kuba M, Nagai H, Yamashita H, Kuba K. β3-Adrenergic activation of sequential Ca²⁺ release from mitochondria and the endoplasmic reticulum and the subsequent Ca²⁺ entry in rodent brown adipocytes. Cell Calcium 2011;49:400-414. https://doi.org/10.1016/j.ceca.2011.02.011

7.   Zhao J, Cannon B, Nedergaard J. Thermogenesis is beta3- but not beta1-adrenergically mediated in rat brown fat cells, even after cold acclimation. Am J Physiol Regul Integr Comp Physiol 1998;275:R2002-R2011. https://doi.org/10.1152/ajpregu.1998.275.6.R2002

8.   Granneman JG. Norepinephrine and BRL37344 stimulate adenylate cyclase by different receptors in rat brown adipose tissue. J Pharmacol Exp Ther 1990;254:508-513.

9.   Nicholls DG, Locke RM. Thermogenic mechanisms in brown fat. Physiol Rev 1984;64:1-64. https://doi.org/10.1152/physrev.1984.64.1.1

10. Trayhurn P. Brown adipose tissue and nutritional energetics - where are we now? Proc Nutr Soc 1989;48:165-175. https://doi.org/10.1079/PNS19890026

11. Klingenberg M, Huang SG. Structure and function of the uncoupling protein from brown adipose tissue. Biochim Biophys Acta 1999;1415:271-296. https://doi.org/10.1016/S0005-2736(98)00232-6

12. Lowell BB, Spiegelman BM. Towards a molecular understanding of adaptive thermogenesis. Nature 2000;404:652-660. https://doi.org/10.1038/35007527

13. Ricquier D, Bouillaud F. Mitochondrial uncoupling proteins: from mitochondria to the regulation of energy balance. J Physiol 2000;529:3-10. https://doi.org/10.1111/j.1469-7793.2000.00003.x

14. Lee SC, Nuccitelli R, Pappone PA. Adrenergically activated Ca2+ increases in brown fat cells: effects of Ca2+, K+, and K channel block. Am J Physiol 1993;264:C217-C228. https://doi.org/10.1152/ajpcell.1993.264.1.C217

15. Nånberg E, Putney J Jr. Alpha1-adrenergic activation of brown adipocytes leads to an increased formation of inositol polyphosphates. FEBS Lett 1986;195:319-322. https://doi.org/10.1016/0014-5793(86)80185-5

16. Omatsu-Kanbe M, Matsuura H. Inhibition of store-operated Ca²⁺ entry by extracellular ATP in rat brown adipocytes. J Physiol 1999;521:601-615. https://doi.org/10.1111/j.1469-7793.1999.00601.x

17. Kuba M, Higure Y, Susaki H, Hayato R, Kuba K. Bidirectional Ca²⁺ coupling of mitochondria with the endoplasmic reticulum and regulation of multimodal Ca²⁺ entries in rat brown adipocytes. Am J Physiol Cell Physiol 2007;292:C896-C908. https://doi.org/10.1152/ajpcell.00649.2005

18. de Meis L, Ketzer LA, da Costa RM, de Andrade IR, Marlene Benchimol M. Fusion of the endoplasmic reticulum and mitochondrial outer membrane in rats brown adipose tissue: activation of thermogenesis by Ca²⁺. PLoS One 2010;5:e9439. https://doi.org/10.1371/journal.pone.0009439

19. Guarnieri AR, Benson TW, Tranter M. Calcium cycling as a mediator of thermogenic metabolism in adipose tissue. Mol Pharmacol 2022;102:51-59. https://doi.org/10.1124/molpharm.121.000465

20. Wolfrum C, Kiehlmann E, Pelczar P. TRPC1 regulates brown adipose tissue activity in a PPARγ-dependent manner. Am J Physiol Endocrinol Metab 2018;315:E825-E832. https://doi.org/10.1152/ajpendo.00170.2017

21. Sukumar P, Sedo A, Li J, Wilson LA, O'Regan D, Lippiat JD, Porter KE, ET AL. Constitutively Active TRPC Channels of Adipocytes Confer a Mechanism for Sensing Dietary Fatty Acids and Regulating Adiponectin. Circ Res 2012;111:191-200. https://doi.org/10.1161/CIRCRESAHA.112.270751

22. Lu W, Wang J, Shimoda LA, Sylvester JT. Differences in STIM1 and TRPC expression in proximal and distal pulmonary arterial smooth muscle are associated with differences in Ca²⁺ responses to hypoxia. Am J Physiol Lung Cell Mol Physiol 2008;295:L104-L113. https://doi.org/10.1152/ajplung.00058.2008

23. Wang J, Weigand L, Lu W, Sylvester JT, Semenza GL, Shimoda LA. Hypoxia inducible factor 1 mediates hypoxia-induced TRPC expression and elevated intracellular Ca²⁺ in pulmonary arterial smooth muscle cells. Circ Res 2006;98:1528-1537. https://doi.org/10.1161/01.RES.0000227551.68124.98

24. Trebak M, Bird GS, McKay RR, Putney JW Jr. Comparison of human TRPC3 channels in receptor-activated and store-operated modes. Differential sensitivity to channel blockers suggests fundamental differences in channel composition. J Biol Chem 2002;277:21617-21623. https://doi.org/10.1074/jbc.M202549200

25. Kanda Y. Investigation of the freely available easy-to-use software 'EZR' for medical statistics. Bone Marrow Transplant 2013;48:452-458. https://doi.org/10.1038/bmt.2012.244

26.   Hu HZ, Gu Q, Wang C, Colton CK, Tang J, Kinoshita-Kawada M, Lee LY, Wood JD, Zhu MX. 2-aminoethoxydiphenyl borate is a common activator of TRPV1, TRPV2, and TRPV3. J Biol Chem 2004;279:35741-35748. https://doi.org/10.1074/jbc.M404164200

27.   Chung MK, Lee H, Mizuno A, Suzuki M, Caterina MJ. 2-aminoethoxydiphenyl borate activates and sensitizes the heat-gated ion channel TRPV3. J Neurosci 2004;24:5177-5182. https://doi.org/10.1523/JNEUROSCI.0934-04.2004

28.   Togashi K, Inada H, Tominaga M. Inhibition of the transient receptor potential cation channel TRPM2 by 2-aminoethoxydiphenyl borate (2-APB). Br J Pharmacol 2008;153:1324-1330. https://doi.org/10.1038/sj.bjp.0707675

29.   Chokshi R, Fruasaha P, Kozak JA. 2-Aminoethyl diphenyl borinate (2-APB) inhibits TRPM7 channels through an intracellular acidification mechanism. Channels 2012;6:362-369. https://doi.org/10.4161/chan.21628

30.   Lievremont JP, Bird GS, Putney JW Jr. Mechanism of inhibition of TRPC cation channels by 2-aminoethoxydiphenylborane. Mol Pharmacol 2005;68:758-762. https://doi.org/10.1124/mol.105.012856

31.   Xu SZ, Zeng F, Boulay G, Grimm C, Harteneck C, Beech DJ. Block of TRPC5 channels by 2-aminoethoxydiphenyl borate: a differential, extracellular and voltage-dependent effect. Br J Pharmacol 2005;145:405-414. https://doi.org/10.1038/sj.bjp.0706197

32.   Shi J, Takahashi S, Jin XH, Li YQ, Ito Y, Mori Y, Inoue R. Myosin light chain kinase-independent inhibition by ML-9 of murine TRPC6 channels expressed in HEK293 cells. Br J Pharmacol 2007;152:122-131. https://doi.org/10.1038/sj.bjp.0707368

33.   Spassova MA, Hewavitharana T, Xu W, Soboloff J, Gill DL. A common mechanism underlies stretch activation and receptor activation of TRPC6 channels. Proc Natl Acad Sci U S A 2006;103:16586-16591. https://doi.org/10.1073/pnas.0606894103

34.   Hofmann T, Obukhov AG, Schaefer M, Harteneck C, Gudermann T, Schultz G. Direct activation of human TRPC6 and TRPC3 channels by diacylglycerol. Nature 1999;397:259-263. https://doi.org/10.1038/16711

35.   Inoue R, Okada T, Onoue H, Hara Y, Shimizu S, Naitoh S, Ito Y, ET AL. The Transient Receptor Potential Protein Homologue TRP6 Is the Essential Component of Vascular alpha1-adrenoceptor-activated Ca2+-Permeable Cation Channel. Circ Res 2001;88:325-332. https://doi.org/10.1161/01.RES.88.3.325

36.   Foster RR, Zadeh MAH, Welsh GI, Satchell SC, Ye Y, Mathieson PW, Bates DO, Saleem MA. Flufenamic acid is a tool for investigating TRPC6-mediated calcium signalling in human conditionally immortalised podocytes and HEK293 cells. Cell Calcium 2009;45:384-390. https://doi.org/10.1016/j.ceca.2009.01.003

37.   Semtner S, Schaefer M, Pinkenburg O, Plant TD. Potentiation of TRPC5 by protons. J Biol Chem 2007;282:33868-33878. https://doi.org/10.1074/jbc.M702577200

38.   Tai Y, Feng S, Ge R, Du W, Zhang X, He Z, Wang Y. TRPC6 channels promote dendritic growth via the CAMKIV-CREB pathway. J Cell Sci 2008;121:2301-2307. https://doi.org/10.1242/jcs.026906

39.   Zhou J, Du W, Zhou K, Tai Y, Yao H, Jia Y, Ding Y, ET AL. Critical role of TRPC6 channels in the formation of excitatory synapses. Nat Neurosci 2008;11:741-743. https://doi.org/10.1038/nn.2127

40.   Jia Y, Zhou J, Tai Y, Wang Y. TRPC channels promote cerebellar granule neuron survival. Nat Neurosci 2007;10:559-567. https://doi.org/10.1038/nn1870

41.   Kunert-Keil C, Bisping F, Krüger J, Brinkmeier H. Tissue-specific expression of TRP channel genes in the mouse and its variation in three different mouse strains. BMC Genomics 2006;7:159. https://doi.org/10.1186/1471-2164-7-159

42.   Wang Y, Falting JM, Mattsson CL, Holmstrom TE, Nedergaard J. In brown adipocytes, adrenergically induced beta(1)-/beta(3)-(Gs)-, alpha(2)-(Gi)- and alpha(1)-(Gq)-signalling to Erk1/2 activation is not mediated via EGF receptor transactivation. Exp Cell Res 2013;319:2718-2727. https://doi.org/10.1016/j.yexcr.2013.08.007

43.   Bishnoi M, Kondepudi KK, Gupta A, Karmase A, Boparai RK. Expression of multiple Transient Receptor Potential channel genes in murine 3T3-L1 cell lines and adipose tissue. Pharmacol Rep 2013;65:751-755. https://doi.org/10.1016/S1734-1140(13)71055-7

44.   Sun W, Uchida K, Suzuki Y, Zhou Y, Kim M, Takayama Y, Takahashi N, ET AL. Lack of TRPV2 impairs thermogenesis in mouse brown adipose tissue. EMBO Rep 2016;17:383-399. https://doi.org/10.15252/embr.201540819

45.   Gottlieb P, Folgering J, Maroto R, Raso A, Wood TG, Kurosky A, Bowman C, ET AL. Revisiting TRPC1 and TRPC6 mechanosensitivity. Pflugers Arch 2008;455:1097-1103. https://doi.org/10.1007/s00424-007-0359-3